Supporting informantion

Crystal Engineering of Ferrocene-Based Charge-Transfer Complexes for NIR-II Photothermal Therapy and Ferroptosis

Wei Ge,[a] Chao Liu,[a] Yatao Xu,[a] Jiayao Zhang,[a] Weili Si,*[a] Wenjun Wang,[b] Changjin Ou,*[c] Xiaochen Dong*[a,d]

[a]Key Laboratory of Flexible Electronics (KLOFE) & Institute of Advanced Materials(IAM), Nanjing Tech University (NanjingTech), 30 South Puzhu Road, Nanjing 211816, China.

E-mail: iamwlsi@njtech.edu.cn

[b]School of Physical Science and Information Technology, Liaocheng University, Liaocheng 252059, China.

[c]School of Chemistry and Materials Science, Nanjing University of Information Science & Technology, Nanjing 210044, China.

E-mail: ocj1987@163.com

[d]School of Chemistry & Materials Science, Jiangsu Normal University, Xuzhou, 221116, China.

E-mail: iamxcdong@njtech.edu.cn

1. Experimental sections

1.1 Materials and characterizations

2,3,5,6-tetrafluoro-7,7,8,8-tetracyanoquinodimethane (F4TCNQ) was purchased from TCI. Ferrocene, ferrocenemethanol, (dimethyl amino methyl) ferrocene, 2-iodoethanol, methyl iodide, iodoethane, cysteine, glutathione, N-Acety-L-Cysteine, serine, sarcosine, o-phenylenediamine, (4,5-dimethyl-2-thiazolyl)-2,5-diphenyl-2-H-tetrazolium bromide (MTT) were purchased from Adamas-beta Co., Ltd. 3,3',5,5'-tetramethylbenzidine (TMB) was obtained from Shanghai Aladdin Bio-Chem Technology Co., Ltd. Cellular lipid peroxides detection kit with Liperfluo was purchased from Dojindo (Shanghai). Reactive oxygen species detection kit (DCFH-DA), glutathione assay kit, JC-1 mitochondrial membrane potential kit and Calcein-AM/PI double stain kit were purchased from Beyotime Biotechnology Co., Ltd.

^{1}H NMR and ^{13}C NMR spectra were measured on Bruker DRX NMR spectrometer with tetramethylsilane (TMS) as the internal standard. X-ray diffraction data for co-crystals were collected on a Bruker APEX-II CCD diffractometer using Mo Kα radiation (λ = 0.71073). P-XRD data were collected with a SmartLab diffractometer. The electron paramagnetic resonance (EPR) spectra were measured by a Bruker A200 (Germany). The absorption spectra were tested on a UV-3600 UV-vis spectrophotometer (Shimadzu, Japan). The sizes and morphologies were tested with SEM S-4800 (Hitachi, Japan) and TEM (JEM-2010FEF). The fluorescence imaging was detected by an inverted fluorescence microscope (Nikon ECLIPSE Ts2R). The temperature variation was recorded by a FLIR thermal camera (E50, Arlington, USA).

1.2 Synthesis of FcN, FcNEt and FcNOH

FcN, FcNEt and FcNOH were all synthesized by salt-forming reaction. For FcN, (dimethyl amino methyl) ferrocene (243 mg, 1 mmol) and methyl iodide (213 mg, 1.5 mmol) was

added into 6 mL diethyl ether for reaction 4 h and generated yellow precipitation which was collected after 3 times centrifugal washing. FcN ^{1}H NMR (300 MHz, DMSO-D6): δ 4.458-4.449 (m, 2H), 4.353-4.351 (m, 4H), 4.209 (s, 5H), 2.869 (s, 9H). ^{13}C NMR (300 MHz, DMSO-D6): δ 73.74, 72.5, 70.55, 69.5, 66.91, 51.90.

Similar procedure was used to synthesize the FcNEt. (dimethyl amino methyl) ferrocene (243 mg, 1 mmol) and iodoethane (234 mg, 1.5 mmol) in 6 mL diethyl ether reacted for 4 h to give yellow precipitation which was collected after 3 times centrifugal washing. FcNEt ^{1}H NMR (300 MHz, DMSO-D6): δ 4.468-4.459 (m, 2H), 4.344-4.328 (m, 4H), 4.219 (s, 5H), 3.177-3.122 (m, 2H), 2.785 (s, 6H), 1.238-1.202 (m, 3H). ^{13}C NMR (300 MHz, DMSO-D6): δ 73.66, 72.63, 70.49, 69.57, 63.97, 58.69, 48.86, 8.46.

For FcNOH, (dimethyl amino methyl) ferrocene (243 mg, 1 mmol) and iodoethane (258 mg, 1.5 mmol) in 6 mL diethyl ether racted for 4 h to generate brown oily which was collected after 3 times centrifugal washing. FcNOH ^{1}H NMR (300 MHz, DMSO-D6): δ 5.2 (s, 1H), 4.49-4.47 (m, 4H), 4.36-4.32 (m, 2H), 4.20 (s, 5H), 3.79 (s, 2H), 3.32 (s, 2H), 2.89 (s, 6H).

1.3 HOMO calculation of Fc-based donors

The highest occupied molecular orbital (HOMO) energy levels of Fc-based donors were calculated based on the following equation:

$$E_{HOMO} = -\left(4.80 - E_{1/2_{Fc/Fc+}} + E_{ox}\right)(eV)$$

where $E_{1/2_{Fc/Fc+}}$ is the redox potential of Fc/Fc^{+} versus Ag/AgCl.

1.4 The preparation and characterization of co-crystals

Co-crystals of these Fc-based donors and F4TCNQ were prepared by the literature method.[1] In short, a solution of the Fc-based donor (0.021 mmol) in $CHCl_3$ (2 mL), a mixture of $CHCl_3$ and CH_2Cl_2 (1:1, 4mL), and a solution of F4TCNQ (0.02 mmol) in CH_2Cl_2 (2 mL) were carefully layered in a test tube and allowed to diffuse for a week. Different crystals precipitated for the X-ray crystallography test. The crystal data and

analyze statistics for those co-crystals are listed in **Table S1** and **S2**.

1.5 Fabrication and characterization of complex nanoparticles

The nanocomplexes of Fc-donors and F4TCNQ were fabricated via the re-precipitation method.[2, 3] Briefly, Fc-donors (10 mmol) and F4TCNQ (10 mmol) were dissolved in 0.3 mL DMSO/THF mixed solution and 0.2 mL THF respectively. Then, the two solutions were mixed and dropped into 9.5 mL DI water under vigorous stirring (prepared in advance) containing poly(ethylene glycol)-block-poly(propylene glycol)-block-poly(ethylene glycol) (F127). The DMSO and THF could be removed by dialysis with 30KDa cut-off membrane, the prepared nanocomplexes were stored in the refrigerator for later use.

1.6 Photothermal performance of ARS NPs

The temperature variation of ARS NPs was measured by a FLIR infrared thermal camera and the photothermal performance was evaluated by changing NPs concentrations (0, 12.5, 25, 50, 100 μg/mL, P = 1.0 W/cm^2) or laser power density (0.2, 0.4, 0.6, 0.8, 1.0, 1.2 W/cm^2, c = 100 μg/mL). And the photothermal conversion efficiency (η) was calculated according to our previous reports.[2] Briefly, the η was calculated based on the following equations:

$$\eta = \frac{hS\Delta T_{max} - Q_s}{I(1 - 10^{-A})}$$

$$\tau_s = \frac{m_D C_D}{hS}$$

where h is the heat transfer coefficient, S is the surface area of the container. τ_s is the sample and system time constant, m_D and C_D are the mass and heat capacity of DI water. ΔT_{max} is the maximum of the temperature changes, Q_s is the heat coming from the DI water when irradiated. I is the laser power density used for nanoparticles irradiation. A is the absorbance of the irradiated nanoparticles at 1060 nm.

The heating/cooling cycle curve were tested under 1060 nm laser irradiation (c = 100

μg/mL, P = 1.2 W/cm^2). The temperature variation was recorded by the thermal camera every 20 seconds.

1.7 Thiols depletion and Fenton reaction abilities of ARS NPs

Thiols (L-cysteine, glutathione, N-Acety-L-Cysteine) depletion ability was tested by a UV-vis-NIR spectrophotometer. Briefly, FcNEt-F4 NPs (FcN-F4 NPs or FcNOH-F4 NPs) (c = 100 μg/mL) and thiols solutions were mixed at room temperature. The absorption spectra were measured at different times. Besides, the absorption spectra of ARS NPS and L-serine (Ser) or sarcosine (Sar) solutions were also recorded.

The Fenton reaction ability of FcNEt-F4 NPs after thiols incubation was tested by a UV-vis-NIR spectrophotometer. When the absorption spectra of FcNEt-F4 NPs and Cys mixture were kept unchanged, OPD or TMB in DMSO solution and H_2O_2 were added and the absorption spectra were tested over time.

1.8 Cells culture

4T1 cancer cells were cultured with a medium containing Roswell Park Memorial Institute (RPMI) 1640, 10% fetal bovine serum (FBS), penicillin (100 U/mL), and streptomycin (100 mg/mL) under a specific environment (containing 5% CO_2 and 37 °C).

1.9 Cytotoxicity assay

4T1 cells were seeded into two 96-well plates and incubated for 24 h. Then the cells were treated with FcNEt-F4 NPs from 0 to 50 μg/mL. One of the plates was irradiated with 1060 nm laser (P = 1 W/cm^2) for 5 min and the other was continued incubating without laser irradiation. After incubating, 20 μL MTT (5 mg/mL) was added for another 4 h and the absorbance at 492 nm in 150 μL DMSO was measured. The cell viability was calculated through the following equation: Cell viability (%) = absorbance of different groups/control group absorbance × 100%.

1.10 Live/dead cells staining experiment

The cells were seeded into 6-well plates and incubated with FcNEt-F4 NPs (40 μg/mL) for 2 h, one of them was irradiated under a 1060 nm laser (P = 1 W/cm^2) for 10 min. The cells were stained with a 2 mL solution of calcein acetoxymethyl ester (calcein AM) and propidium iodide (PI). After washing the cells with PBS, the plates were placed under a fluorescence microscope to observe the green and red fluorescence from calcein AM and PI respectively (calcein AM: 465 nm, PI: 533 nm).

1.11 Total GSH levels in cells

Intracellular total GSH was evaluated by the total GSH assay kit. The GSH lysed from different treatment groups (0, 10, 30, 50 μg/mL) could react with DTNB and the absorption was measured via a microplate reader. The relative GSH levels were calculated through the absorption ratio of different treatment groups and the control group.

1.12 Cellular ROS accumulation and lipid peroxide (LPO) detection

ROS and LPO accumulation was detected by DCFH-DA and Liperfluo respectively. 4T1 cells were seeded into a 6-well plate and incubated with a fresh complement medium for 24 h. Then the cells were treated with FcNEt-F4 NPs of different concentrations (0, 10, 50 μg/mL) and continued to incubate for 2-4 hours. After the incubation, following the instructions, the culture solution was removed and treated with DCFH-DA solution for 20 minutes. Finally, the washed 6-well plate was observed with a fluorescent inverted microscope.

4T1 cells were seeded into a 12-well plate and incubated for 24 h. After 2-4 hours of incubation with various concentrations of FcNEt-F4 NPs (0, 10, 20, 40, 50 μg/mL, 20 μg/mL + laser), the medium was removed and washed with fresh RPMI 1640 (without FBS). Then, 3 μmol/L Liperfluo was added into the wells and waited 30 min and finally washed two times for later observation under a microscope.

1.13 Mitochondrial membrane potential assay with JC-1

After incubation with FcNEt-F4 NPs (0, 20, 30, 40, 50 μg/mL and 30 μg/mL + laser), the 4T1 cells in a 12-well plate were stained with 600 μL JC-1 working solution for 20 min. When the incubation was finished, the cells were washed three times and the JC-1 fluorescence of different treatment groups was observed through a fluorescence microscope.

2. Synthetic routes and characterization of Fc-donors

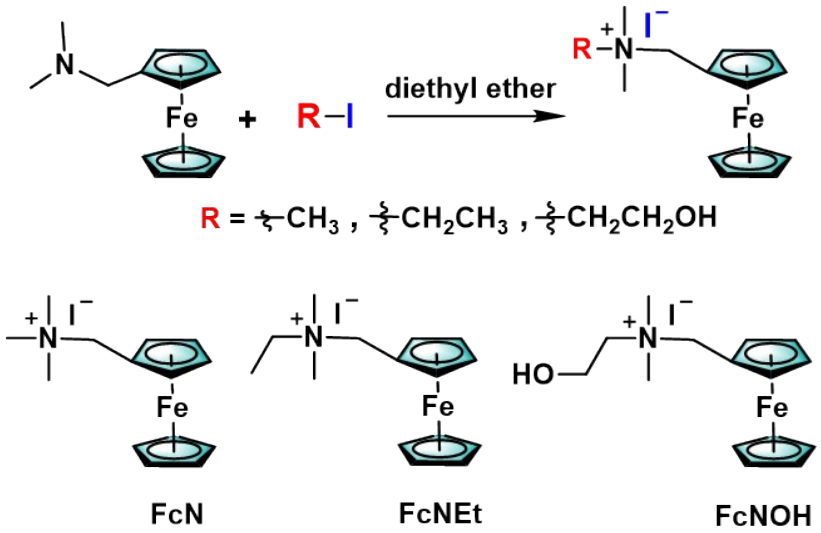

Figure S1. The synthetic route of FcN, FcNEt and FcNOH.

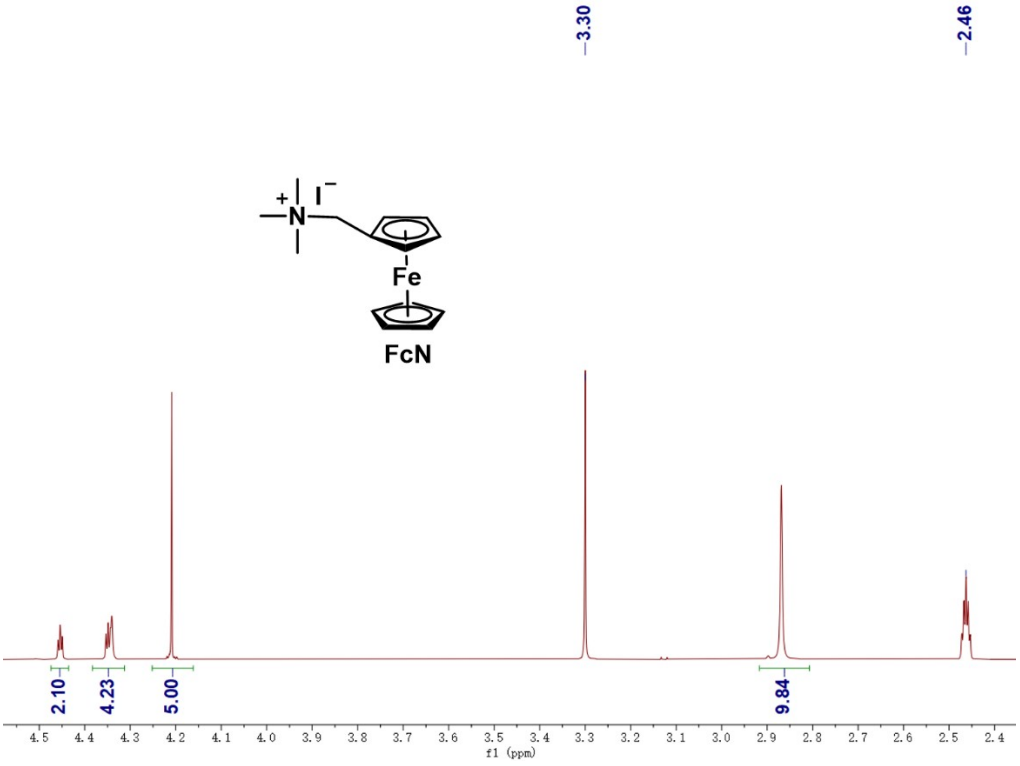

Figure S2. ^{1}H NMR of FcN.

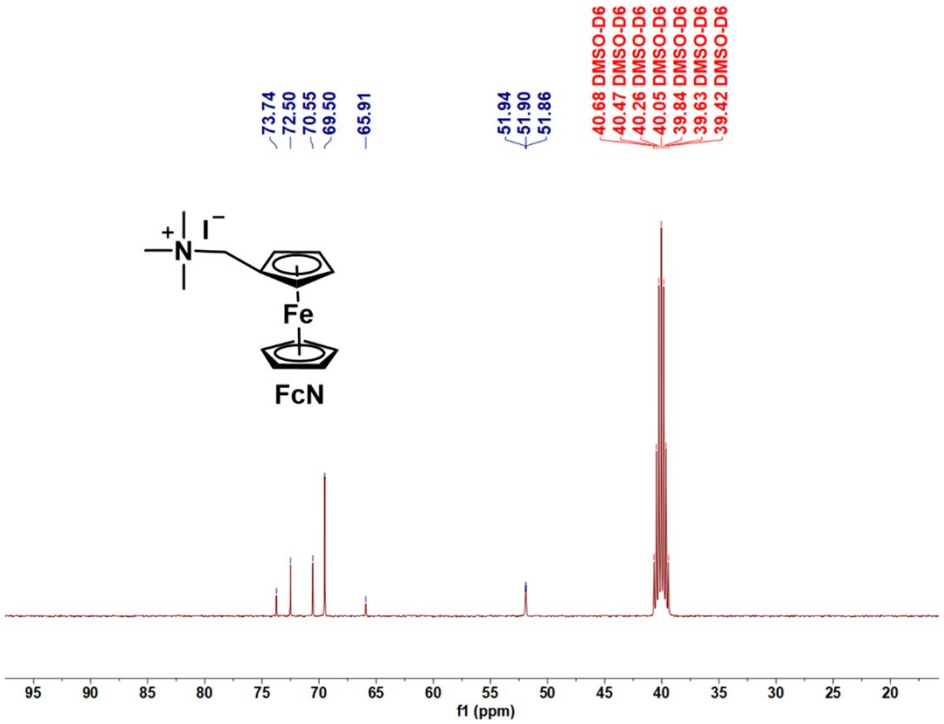

Figure S3. ^{13}C NMR of FcN.

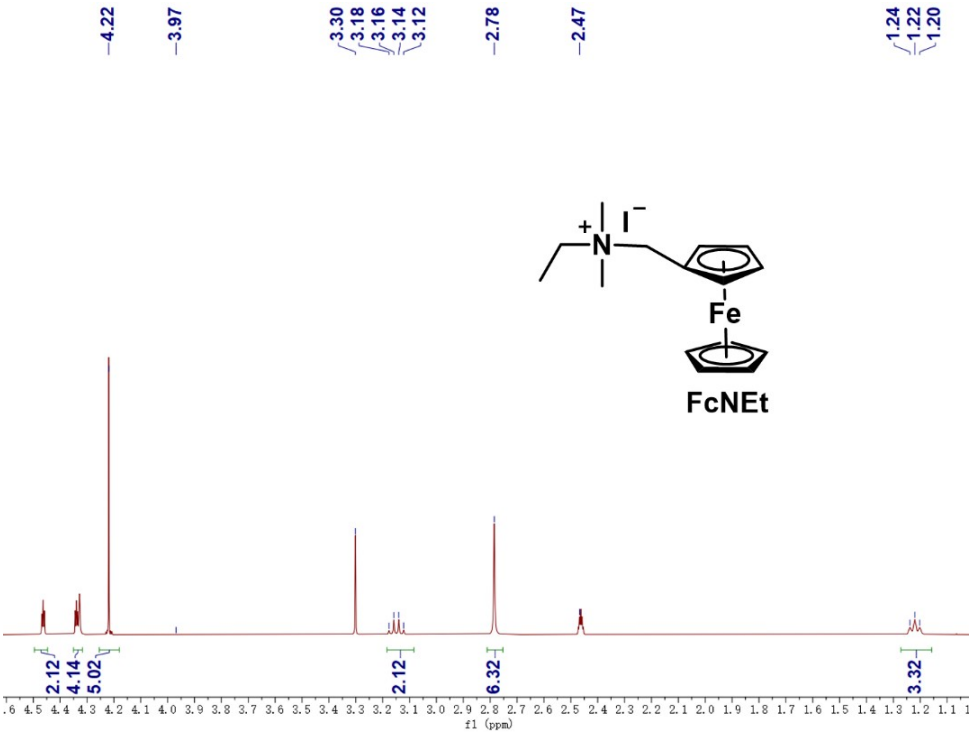

Figure S4. ^{1}H NMR of FcNEt.

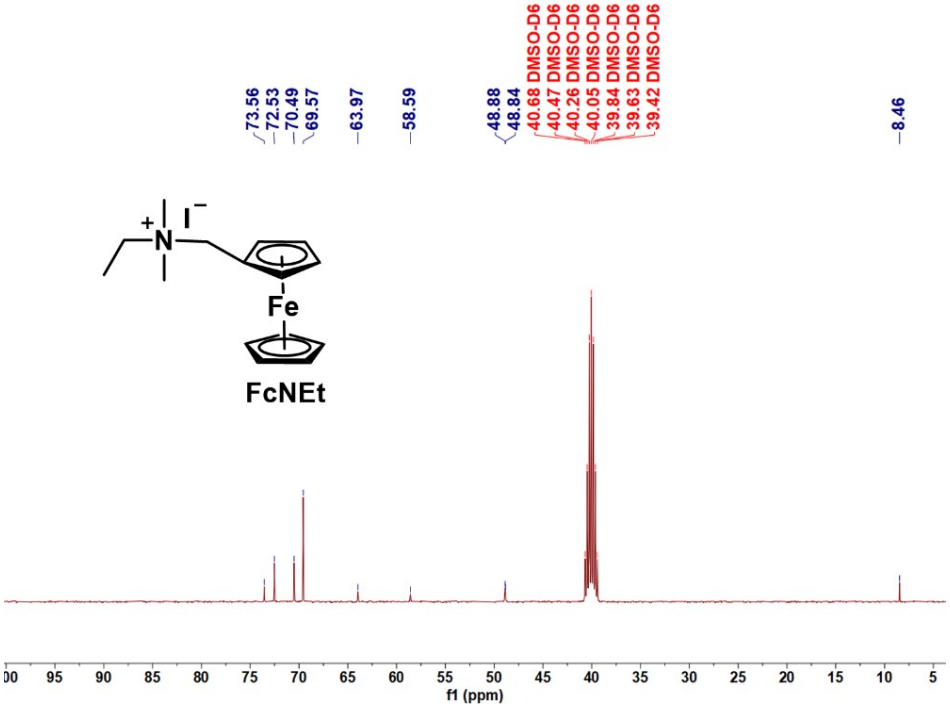

Figure S5. ^{13}C NMR of FcNEt.

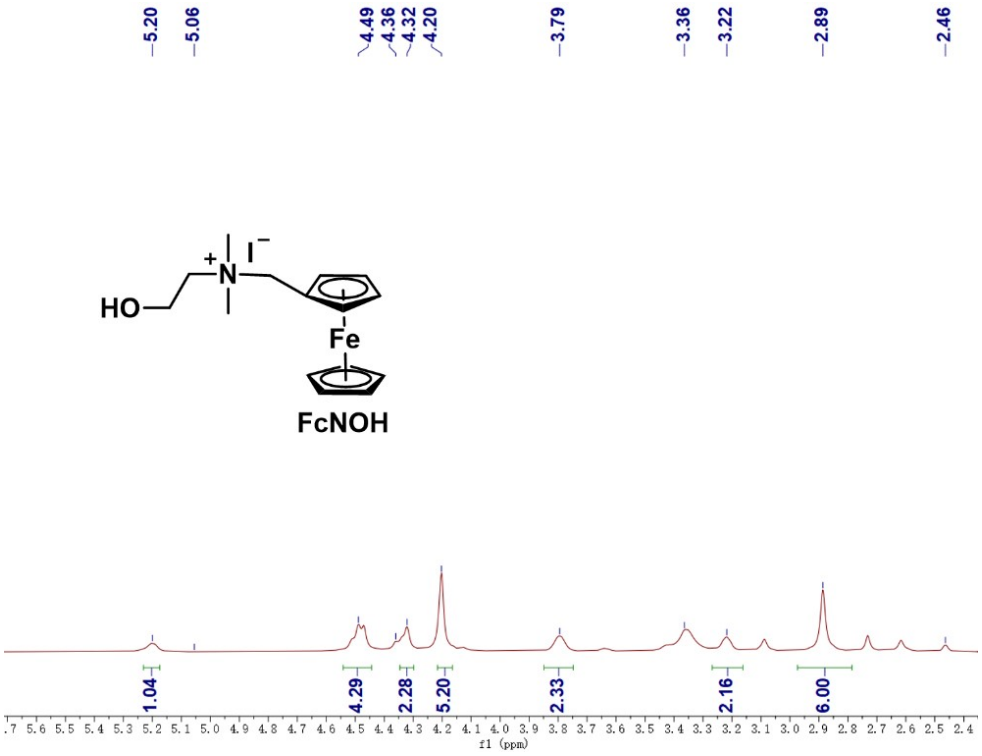

Figure S6. ^{1}H NMR of FcNOH.

3. Additional tables S1, S2, and Figures S7-S32

Table S1. Crystallographic data and some details of data collection and refinement

Compound	**Fc-F4**	**FcOH-F4**	**FcN-F4**	**FcNEt-F4**	**FcNOH-F4**
CCDC No.	2104281	2104286	2104283	2105451	2104284
Empirical formula	$C_{44}H_{20}F_8Fe_2N_8$	$C_{174}H_{66}F_{36}Fe_6N_{36}O_6$	$C_{26}H_{20}F_4FeN_5$	$C_{27}H_{22}F_4FeN_5$	$C_{27}H_{22}F_4FeN_5O$
M [g mol^{-1}]	774.75	3775.72	534.32	548.34	564.34
Crystal system	monoclinic	monoclinic	monoclinic	monoclinic	monoclinic
Space group	*C* 1 2/c 1	*C* 1 2/m 1	*P* 1 2_1/c 1	*P* 1 2_1/c 1	*P* 1 2_1/c 1
a, Å	27.131(5)	25.3524(5)	6.9504(12)	14.3429(8)	23.6772(6)
b, Å	14.624(2)	14.672(3)	24.642(5)	23.932(11)	24.649(6)
c, Å	14.016(3)	22.3122(4)	14.152(4)	14.0730(7)	14.3764(5)
α, deg	90	90	90	90	90
β, deg	117.126(10)	112.3570(10)	98.702(14)	99.514(2)	119.206(10)
γ, deg	90	90	90	90	90
V, Å	4949.3(16)	7675.6(3)	2395.9(9)	4764.3(4)	7323.7(4)
Z value	8	2	4	8	12
ρ_{cal}, g cm^{-3}	2.079	1.634	1.481	1.529	1.535
F(000)	3145	3780	1092	2248	3468
T [K]	296	296	297	150	173
Reflns measured	9087	9943	8628	9915	9249
Parameters	416	655	328	673	1036
Restrains	20	528	0	0	53
$R_1[gt]/wR_2$	0.0332/0.0933	0.0397/0.1295	0.0472/0.1298	0.0680/0.1559	0.1258/0.3077
Goodness of fit	1.044	0.981	1.052	1.209	1.256

Table S2. Crystallographic data of FcNEt-F4 co-crystal at 150 K and 350 K

Compound	**FcNEt-F4 150 K**	**FcNEt-F4 350 K**
Empirical formula	$C_{27}H_{22}F_4FeN_5$	$C_{27}H_{22}F_4FeN_5O$
M [g mol^{-1}]	548.34	564.34
Crystal system	monoclinic	monoclinic
Space group	*P* 1 2_1/c 1	*P* 1 2_1/c 1
a, Å	14.3429(8)	7.1843(14)
b, Å	23.932(11)	24.351(6)
c, Å	14.0730(7)	14.316(3)
α, deg	90	90
β, deg	99.514(2)	97.281(6)
γ, deg	90	90
V, Å	4764.3(4)	2484.3(9)
Z value	8	4
ρ_{cal}, g cm^{-3}	1.529	1.466
F(000)	2248	1124
T [K]	150	350.01
Reflns measured	9915	5789
Parameters	673	374
Restrains	0	87
$R_1[gt]/wR_2$	0.0680/0.1559	0.1290/0.1826
Goodness of fit	1.209	1.232

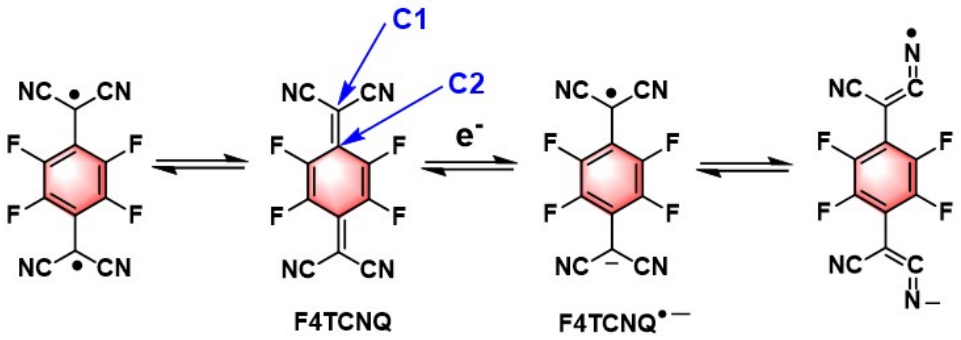

Figure S7. Molecular structures of F4TCNQ and F4TCNQ radical anions and their transformation between radicaloid and quinoid structures.

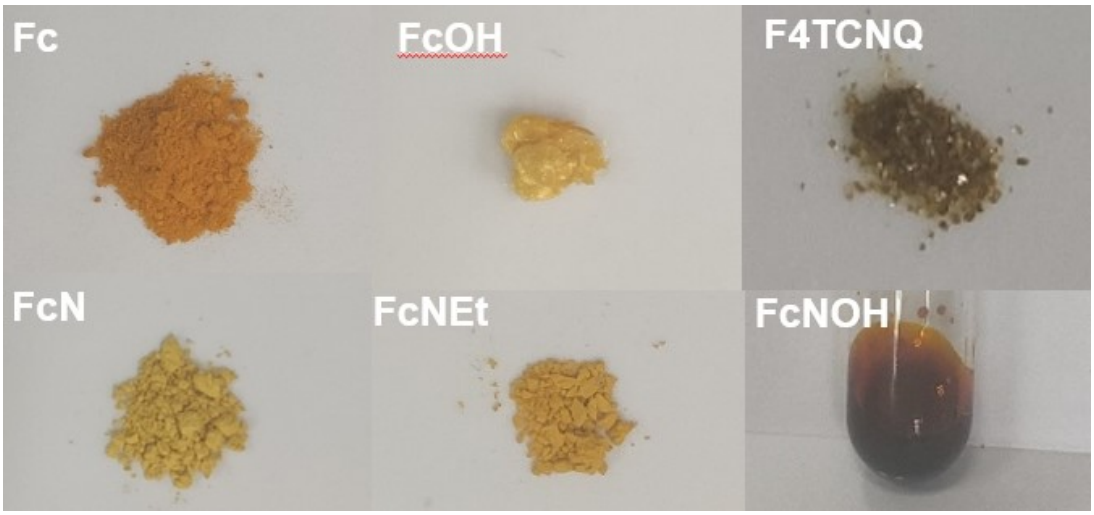

Figure S8. Photographs of the Fc-based donors and F4TCNQ.

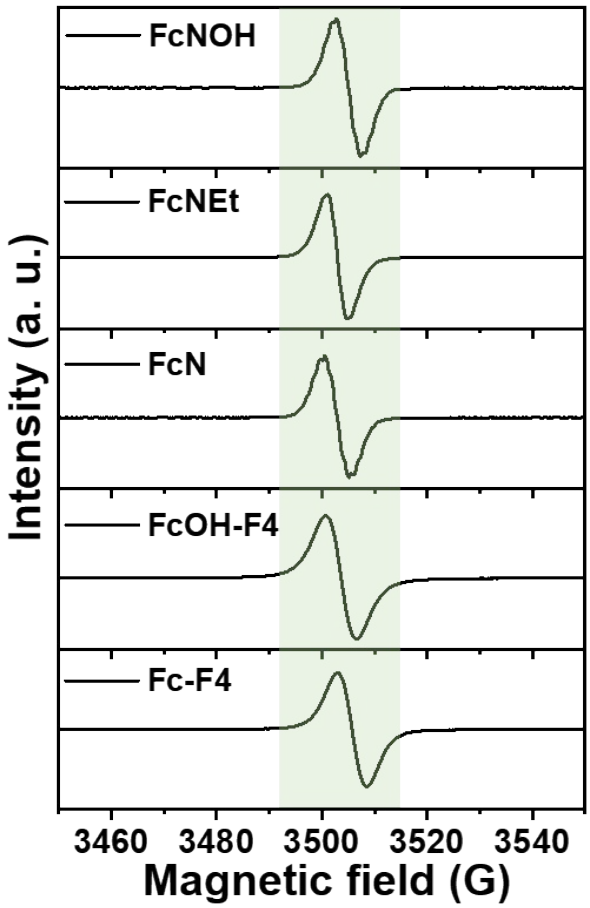

Figure S9. ESR spectra of five Fc-based complexes.

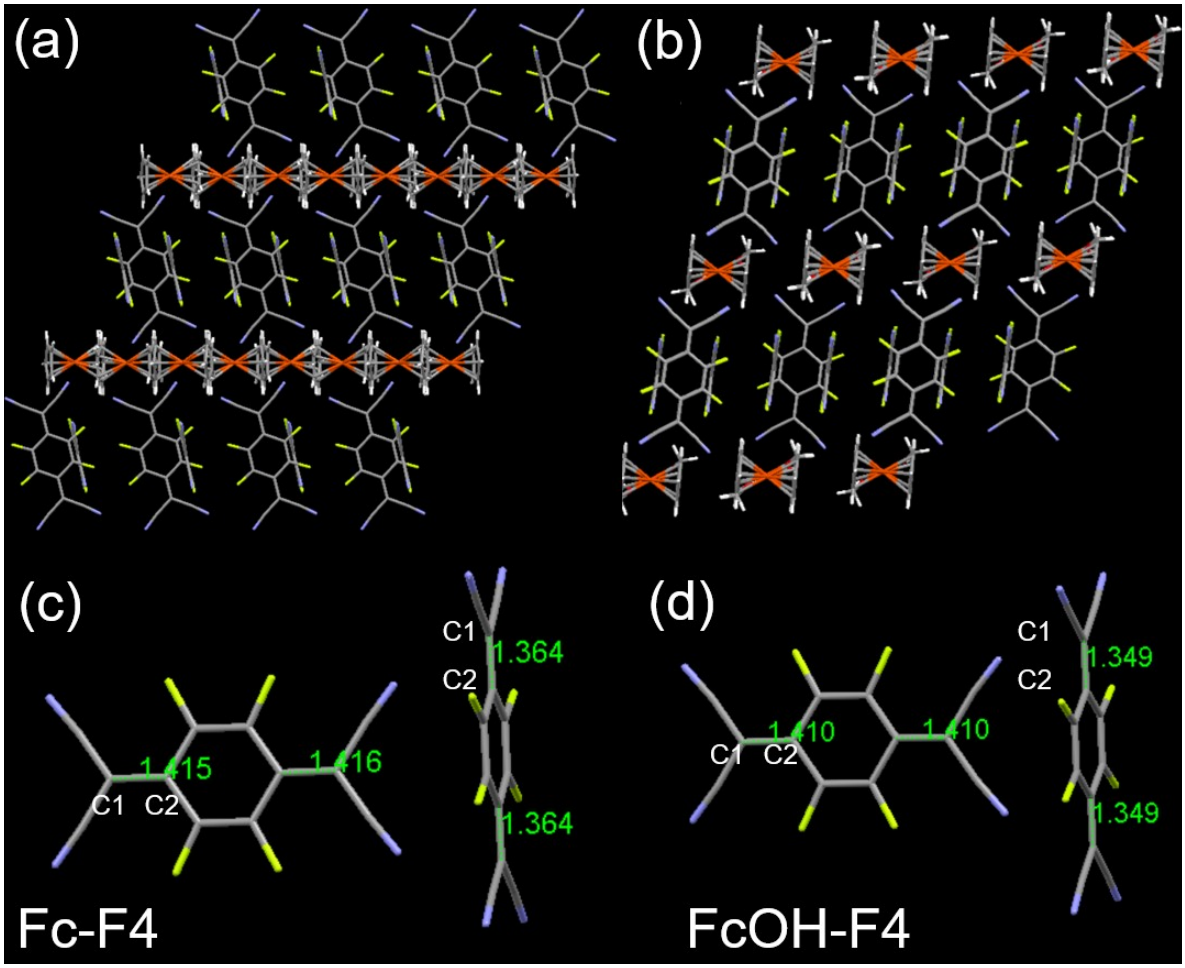

Figure S10. (a, b) Packing diagram of Fc-F4 and FcOH-F4. (c, d) C1-C2 distances measurement in F4TCNQ from co-crystals data.

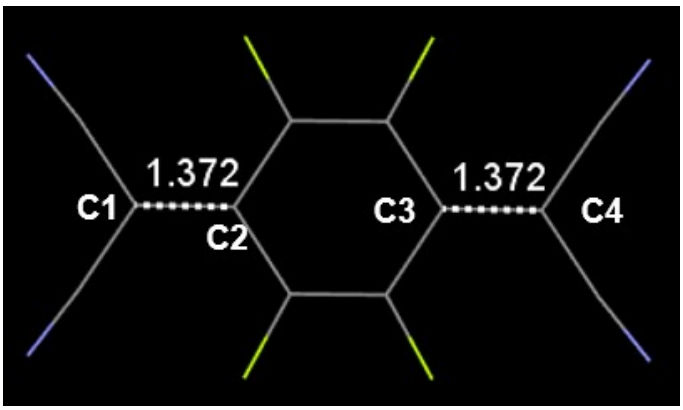

Figure S11. Single crystal data of neutral F4TCNQ and the C1-C2 and C3-C4 distances.

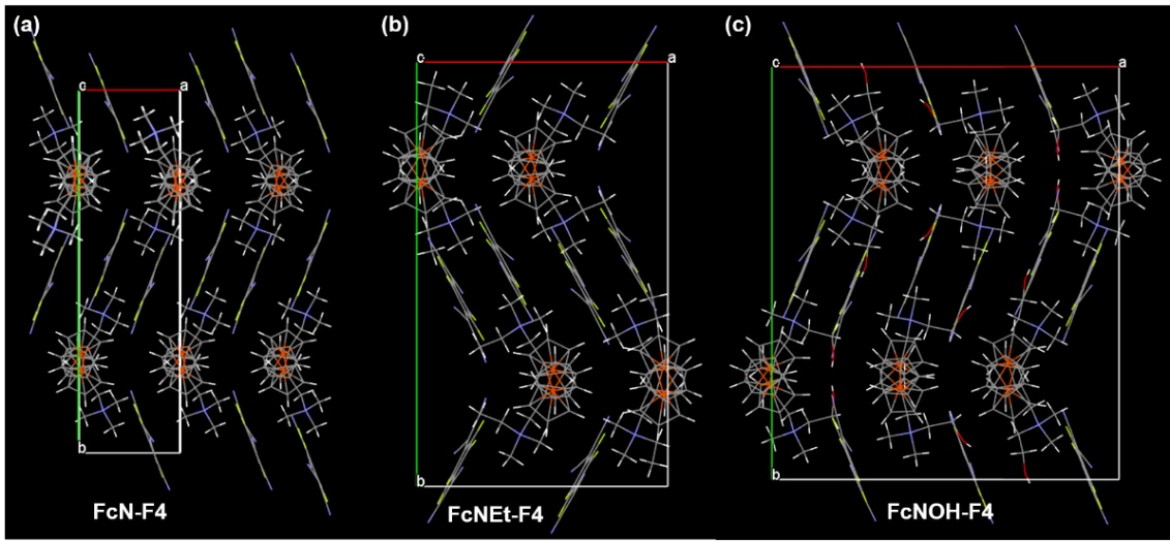

Figure S12. (a-c) The packing diagrams of FcN-F4, FcNEt-F4 and FcNOH-F4.

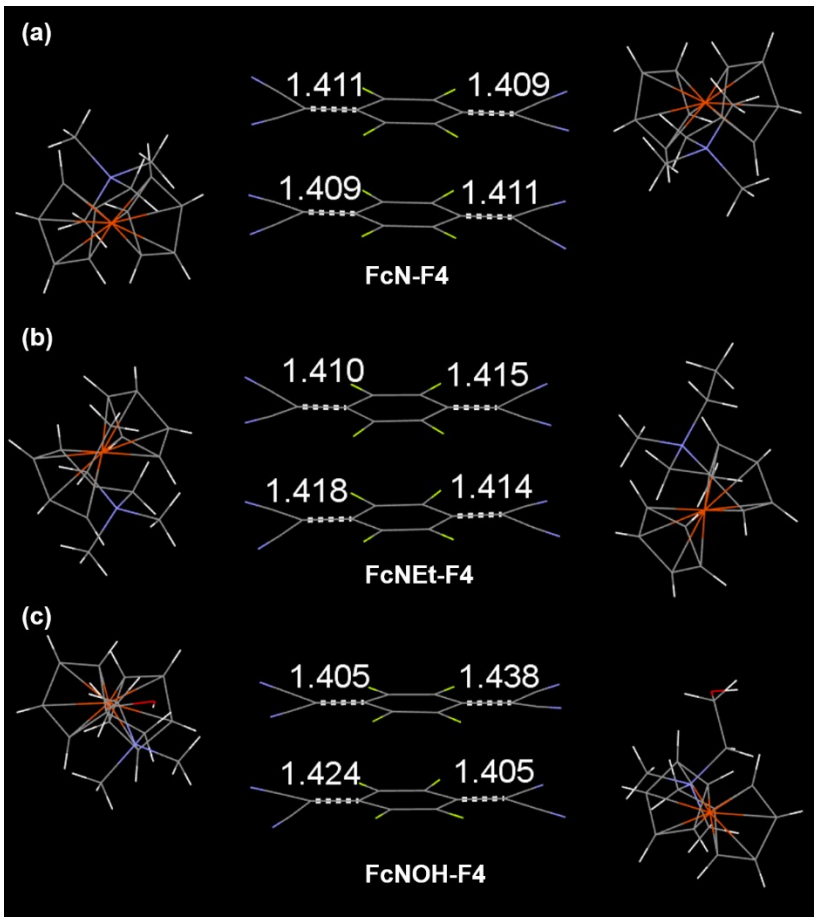

Figure S13. (a-c) C1-C2 distances measurement in F4TCNQ from co-crystals data of FcN-F4, FcNEt-F4 and FcNOH-F4.

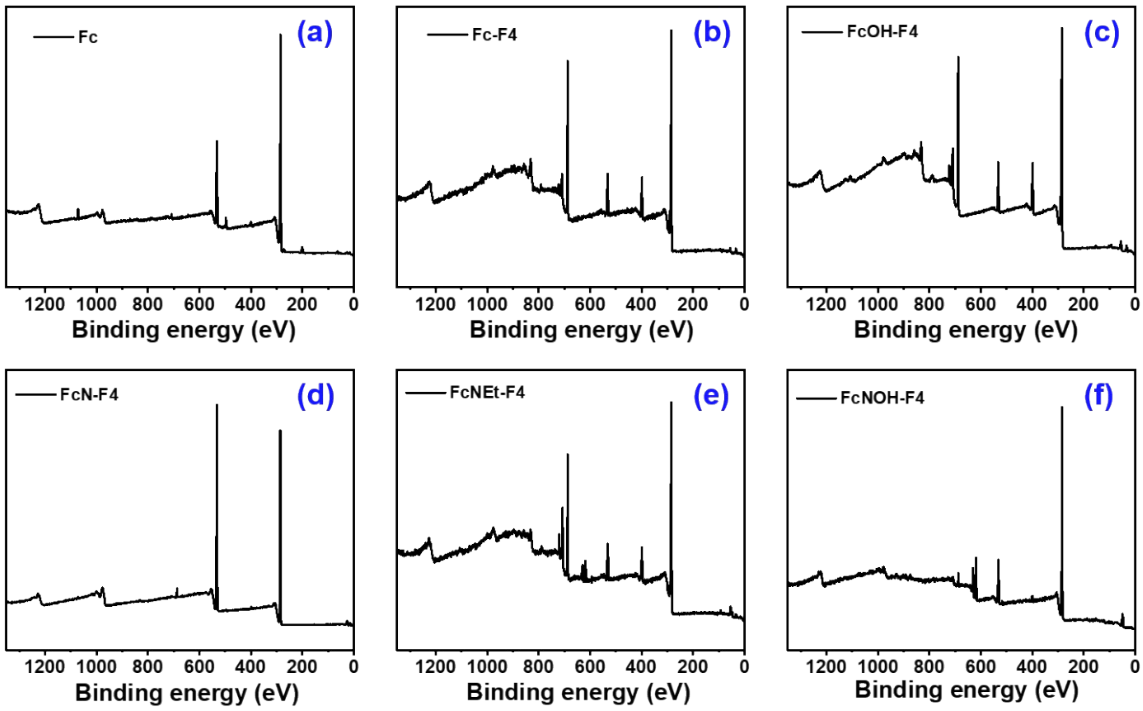

Figure S14. (a-f) Full XPS spectra of Fc, Fc-F4, FcOH-F4, FcN-F4, FcNEt-F4, FcNOH-F4.

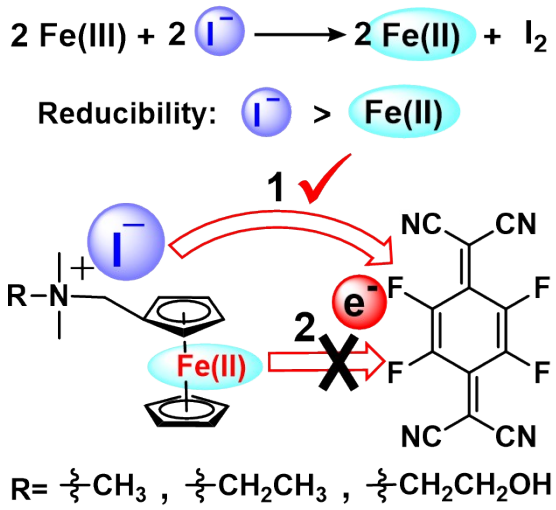

Figure S15. The reaction between Fe(III) and I^- proving the stronger reducibility of I^- than Fe(II) and the charge transfer mechanism in ARSs.

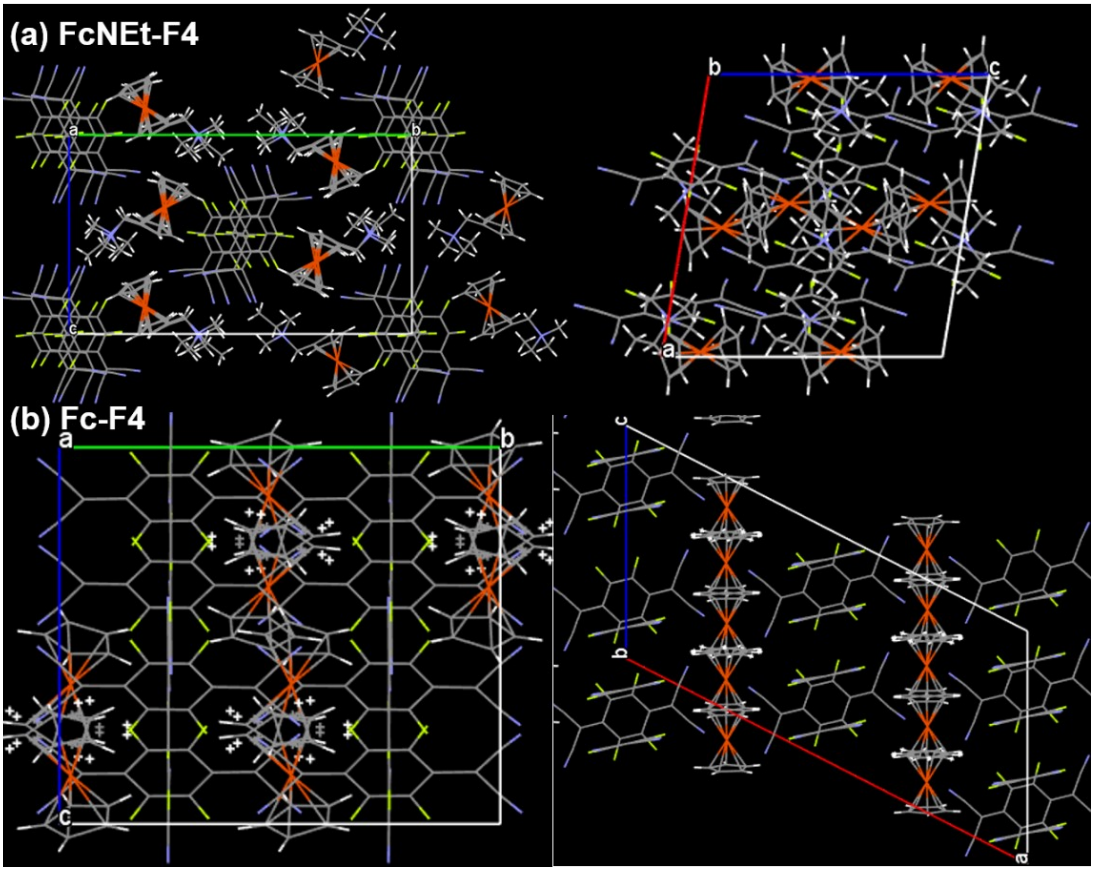

Figure S16. (a) Packing diagrams of FcNEt-F4 from axis a and b. (b) Packing diagrams of Fc-F4 from axis a and b.

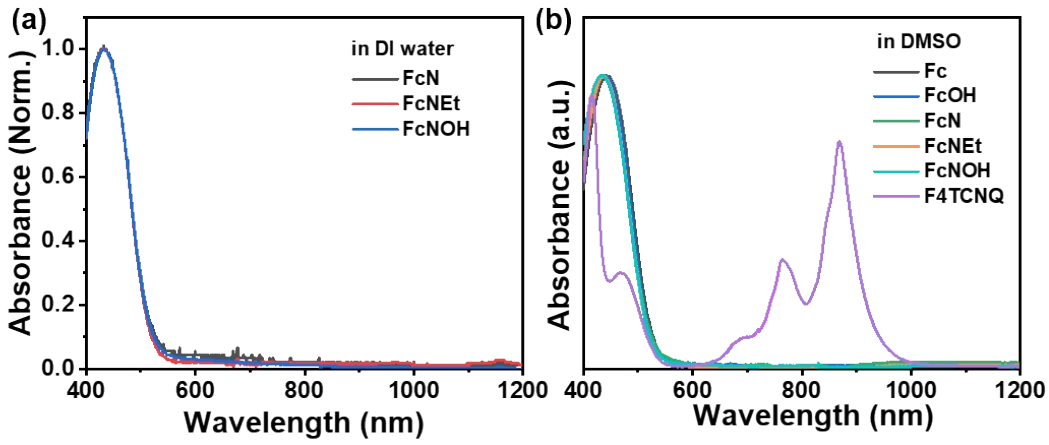

Figure S17. (a) The absorption spectra of FcN, FcNEt and FcNOH in DI water. (b) Absorption spectra of Fc-based donors and F4TCNQ in DMSO.

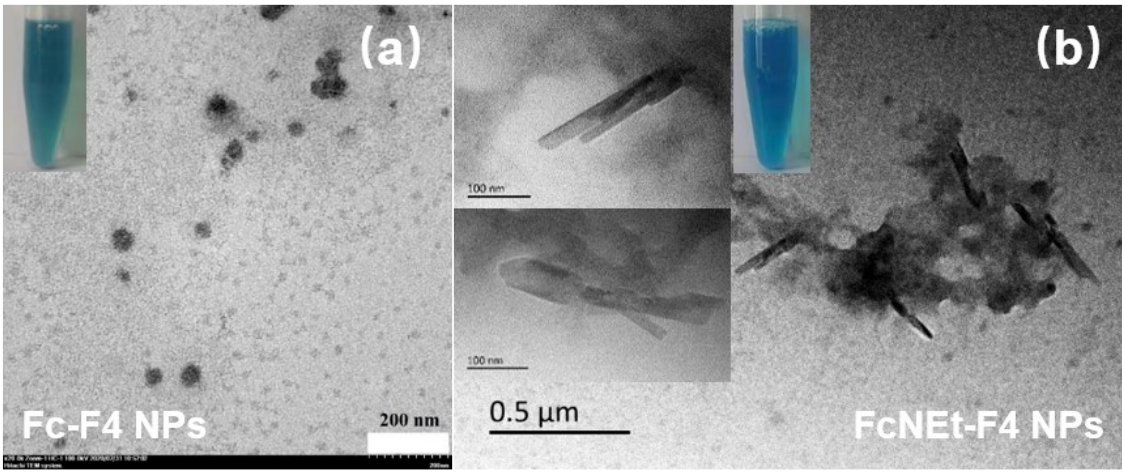

Figure S18. (a, b) Photographs and TEM images of Fc-F4 NPs and FcNEt-F4 NPs.

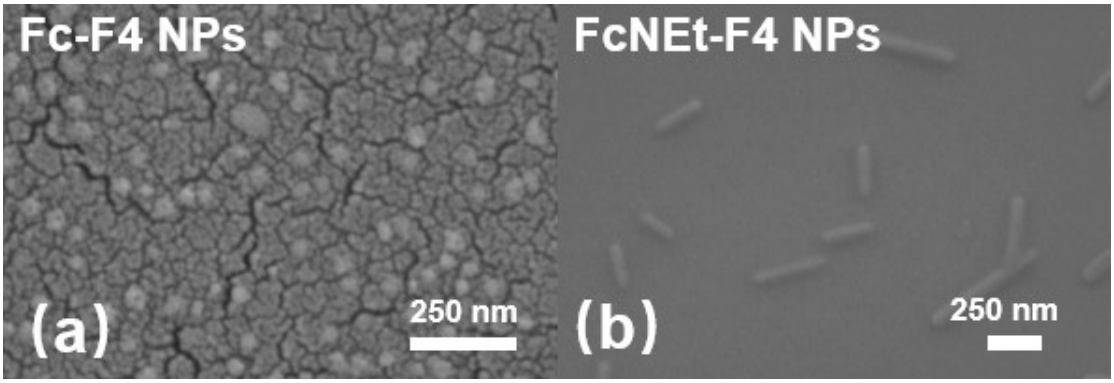

Figure S19. SEM images of Fc-F4 NPs and FcNEt-F4 NPs.

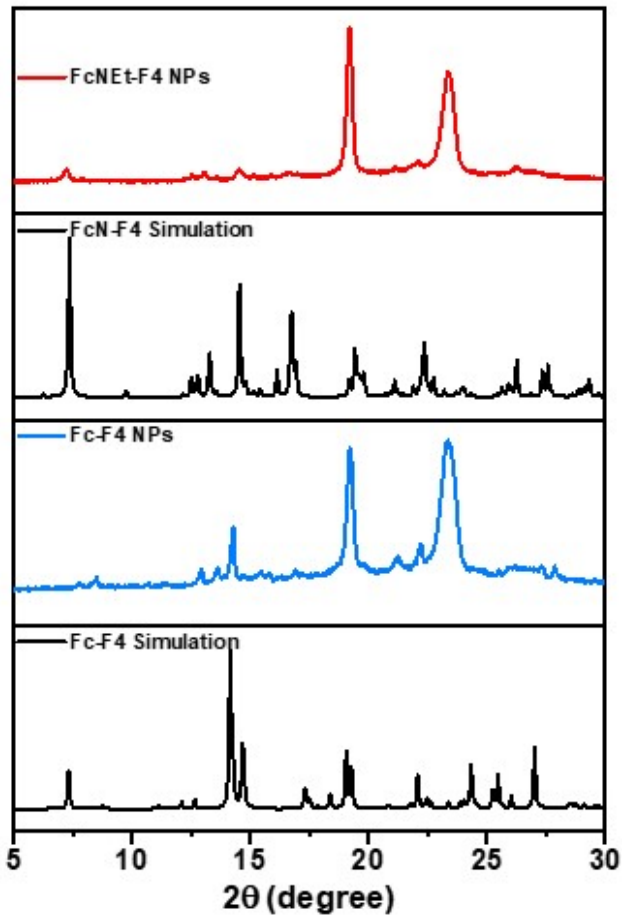

Figure S20. XRD data of Fc-F4 NPs and FcNEt-F4 NPs from freeze-dried powders and co-crystals simulation data.

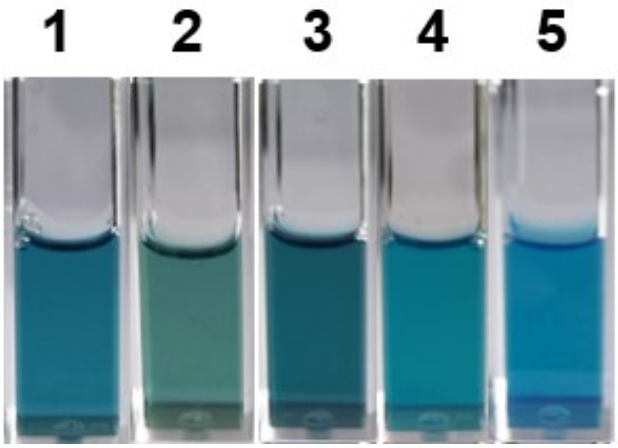

Figure S21. The photographs of Fc-based nanoparticles (1-5 are Fc-F4, FcOH-F4, FcN-F4, FcNEt-F4 and FcNOH-F4 NPs, respectively).

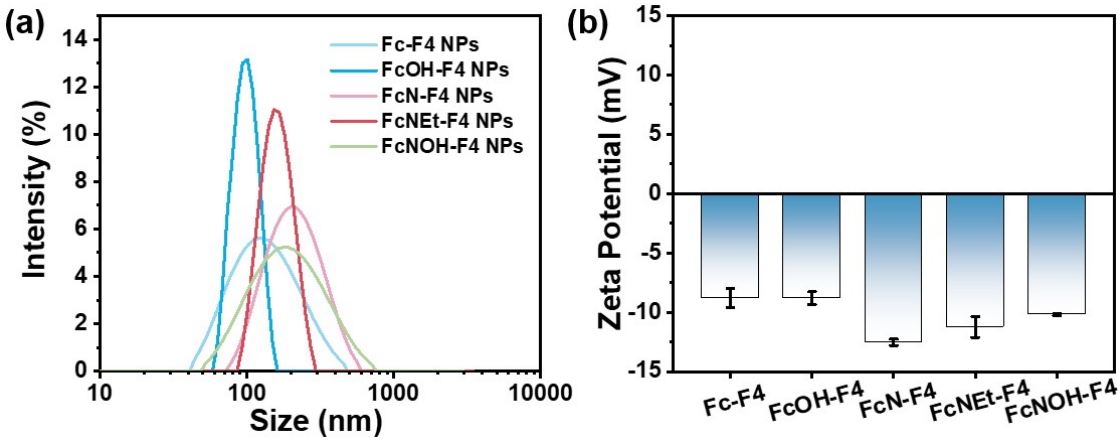

Figure. S22. (a, b) DLS and zeta potential data of Fc-based nanoparticles (Fc-F4, FcOH-F4, FcN-F4, FcNEt-F4 and FcNOH-F4 NPs).

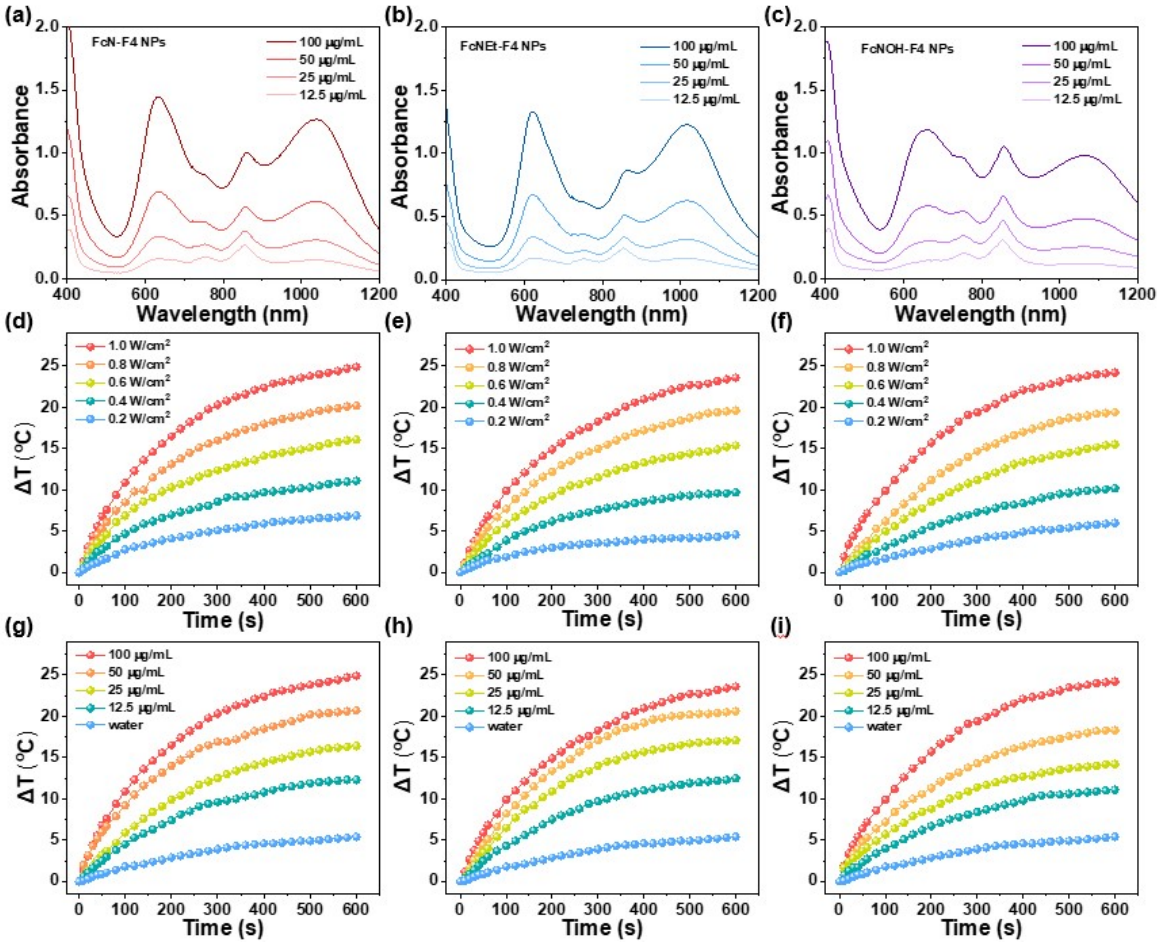

Figure S23. (a-c) The absorption spectra of FcN-F4, FcNEt-F4 and FcNOH-F4 NPs at different concentrations (12.5, 25, 50, 100 μg/mL). (d-f) The temperature variation of FcN-F4, FcNEt-F4 and FcNOH-F4 NPs with the power density from 0.2 to 1.0 W/cm^2 (c = 100 μg/mL). (g-i) The temperature variation of FcN-F4, FcNEt-F4 and FcNOH-F4 NPs with the concentration from 0 to 100 μg/mL (P = 1.0 W/cm^2).

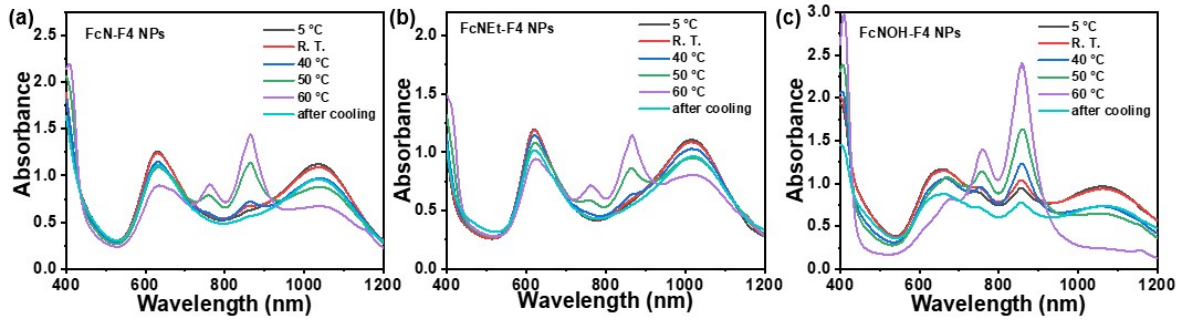

Figure S24. (a-c) The absorption spectra of FcN-F4 NPs, FcNEt-F4 NPs and FcNOH-F4 NPs at different temperature.

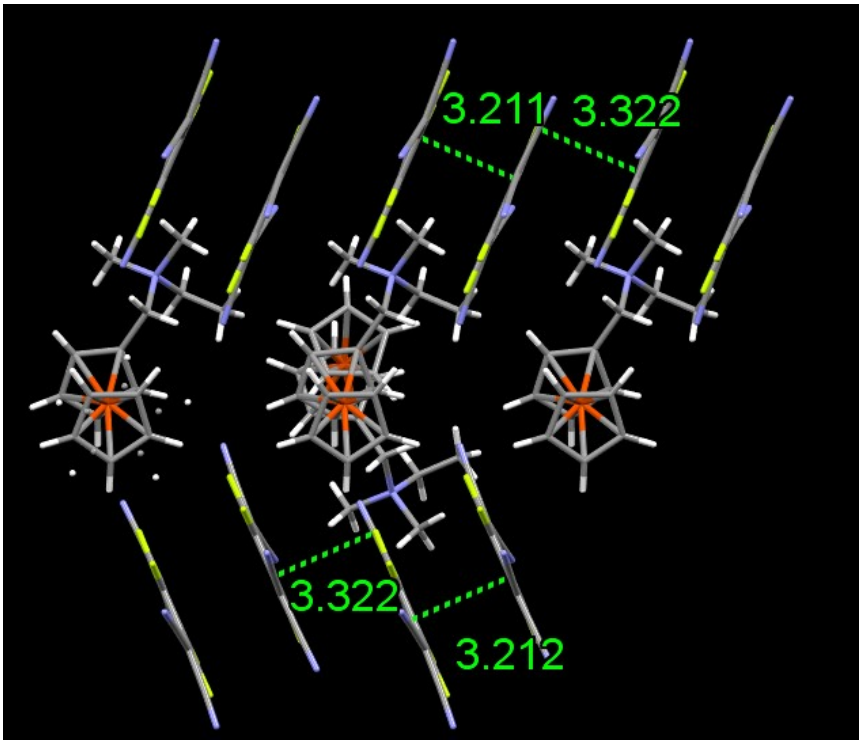

Figure S25. The crystal data of FcNEt-F4 at 350 K and the distances between F4TCNQ.

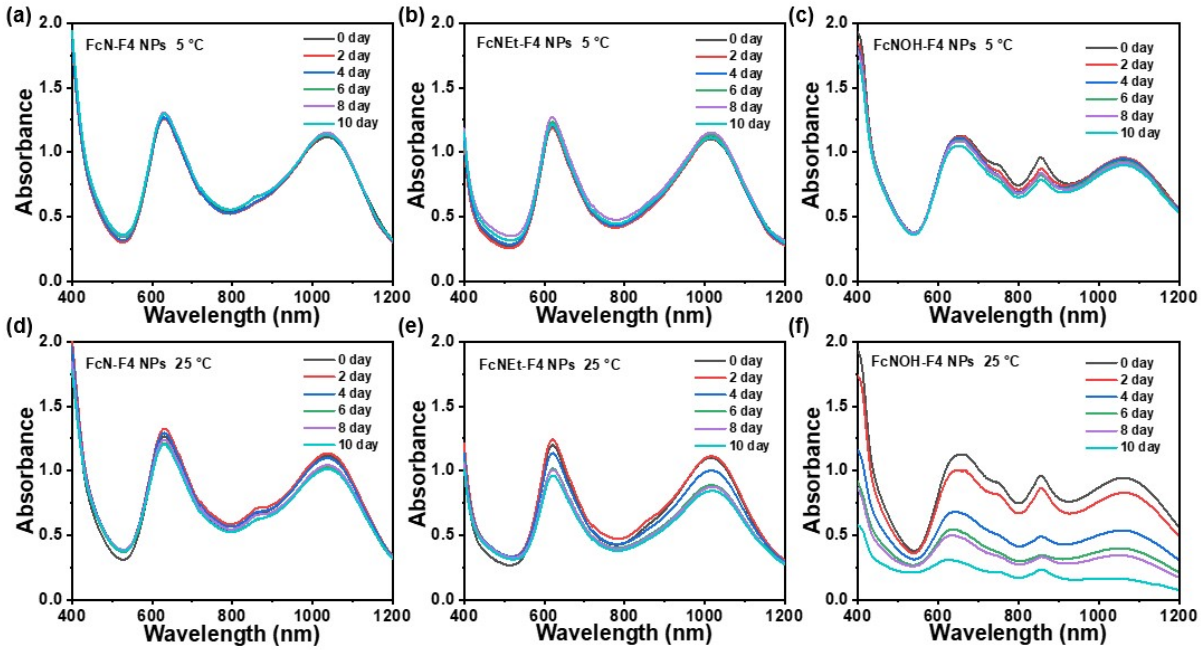

Figure S26. The absorption spectra of FcN-F4 NPs, FcNEt-F4 NPs and FcNOH-F4 NPs recorded from 0 to day 10 at different temperature (5 and 25 °C).

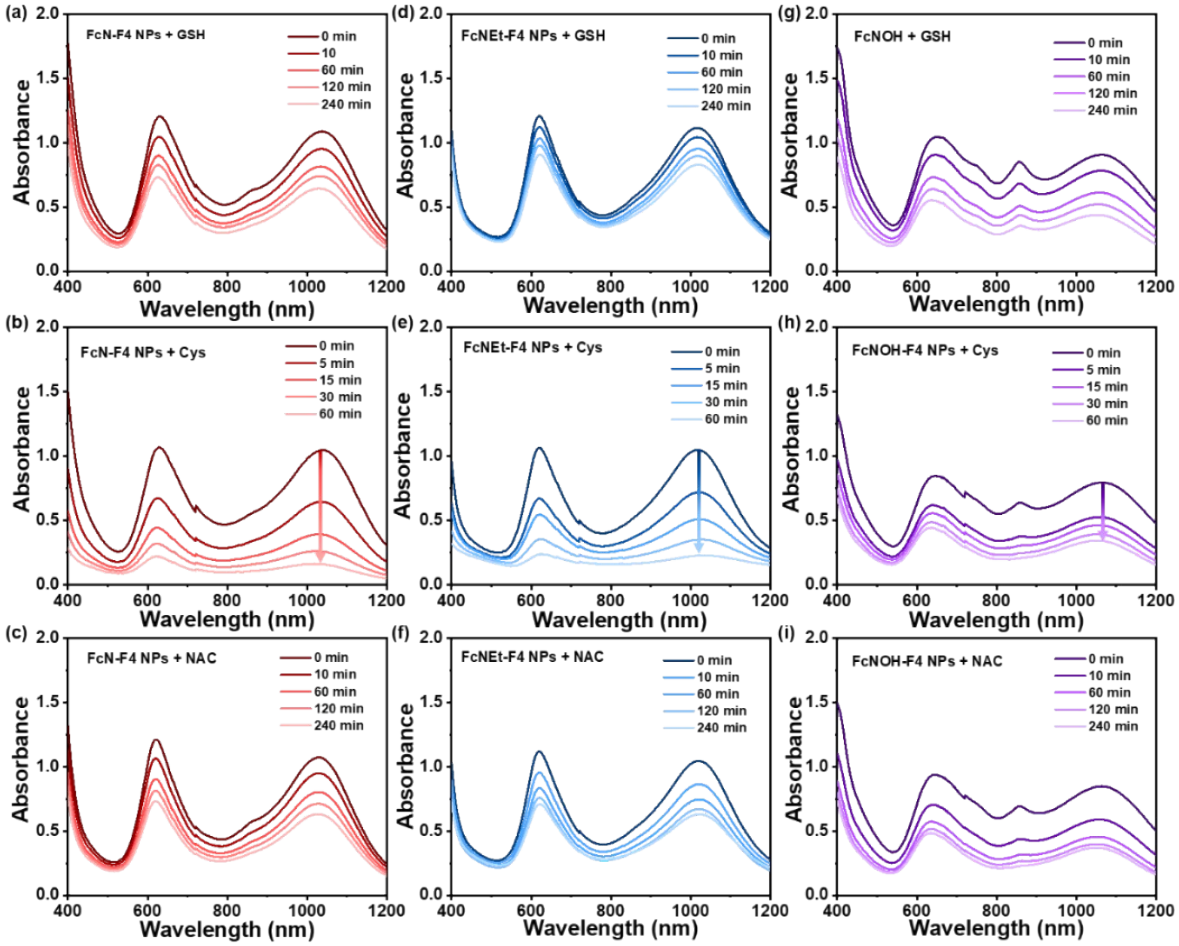

Figure S27. (a-i) The absorption spectra at different time of three ARS NPs (100 μg/mL) incubated with GSH, Cys, NAC solutions (red, blue and purple represent FcN-F4 NPs, FcNEt-F4 NPs and FcNOH-F4 NPs respectively).

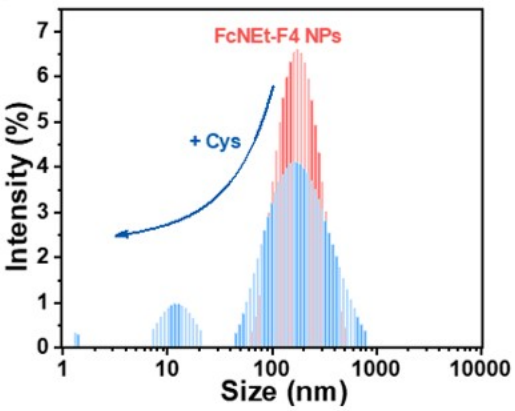

Figure S28. DLS data of FcNEt-F4 NPs before and after incubation with Cys solution.

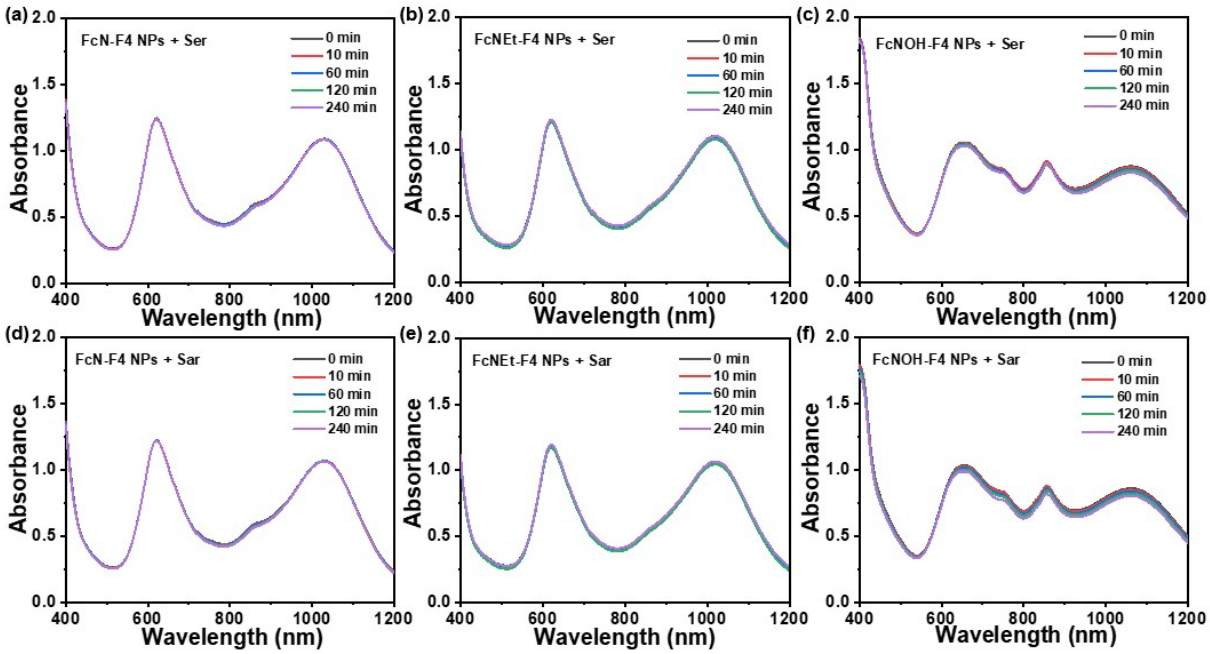

Figure S29. The absorption spectra at different time of three ARS NPs (100 μg/mL) incubated with Ser and Sar solutions.

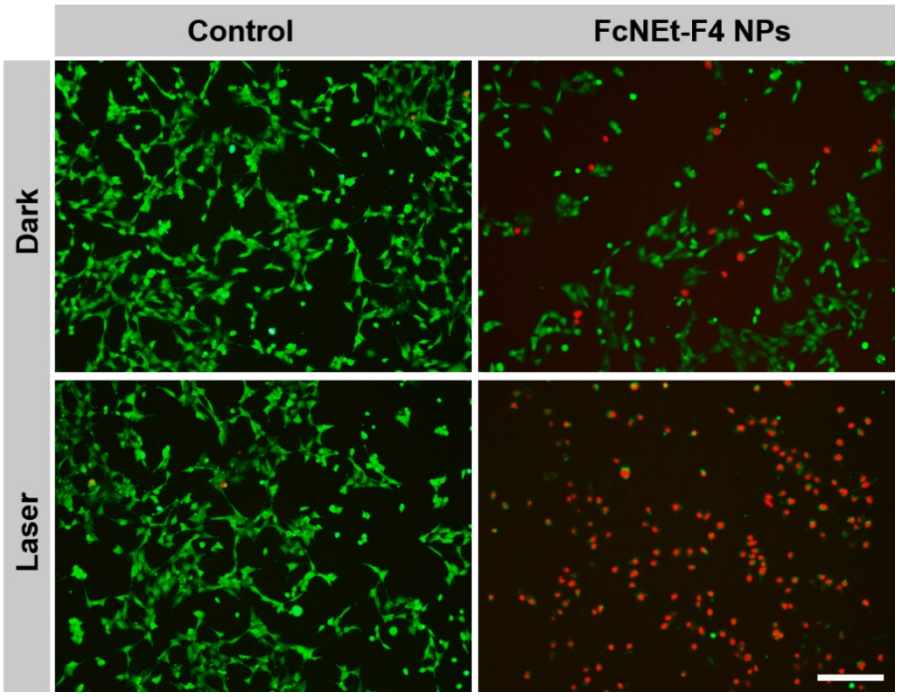

Figure S30. Live/dead staining images with different treatments (c = 40 μg/mL).

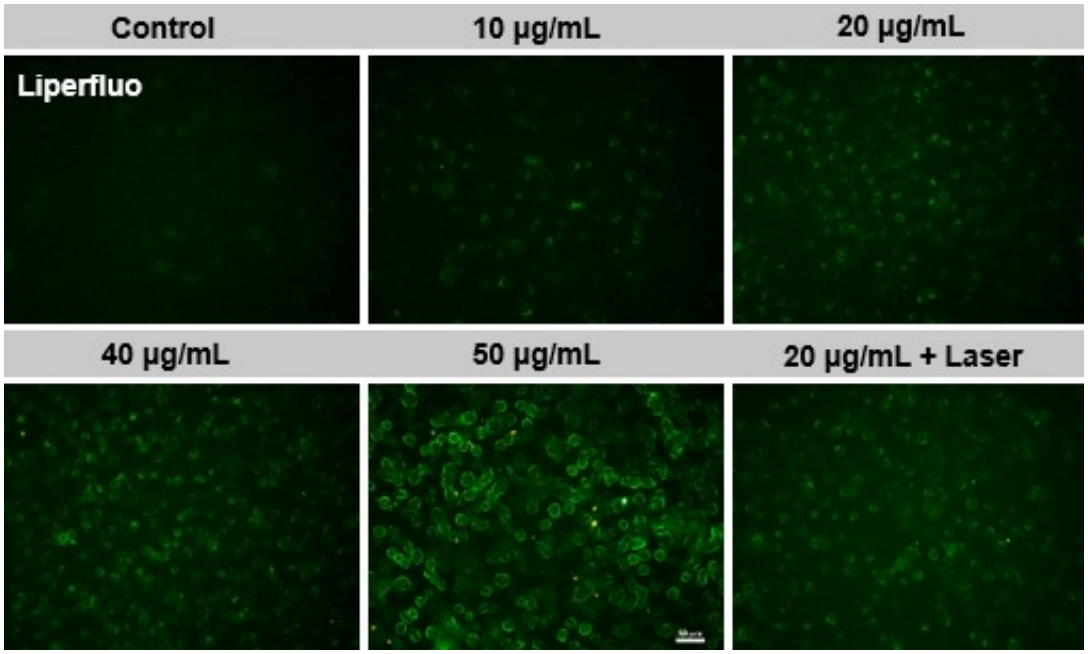

Figure S31. LPO staining images of 4T1 cells after different treatments.

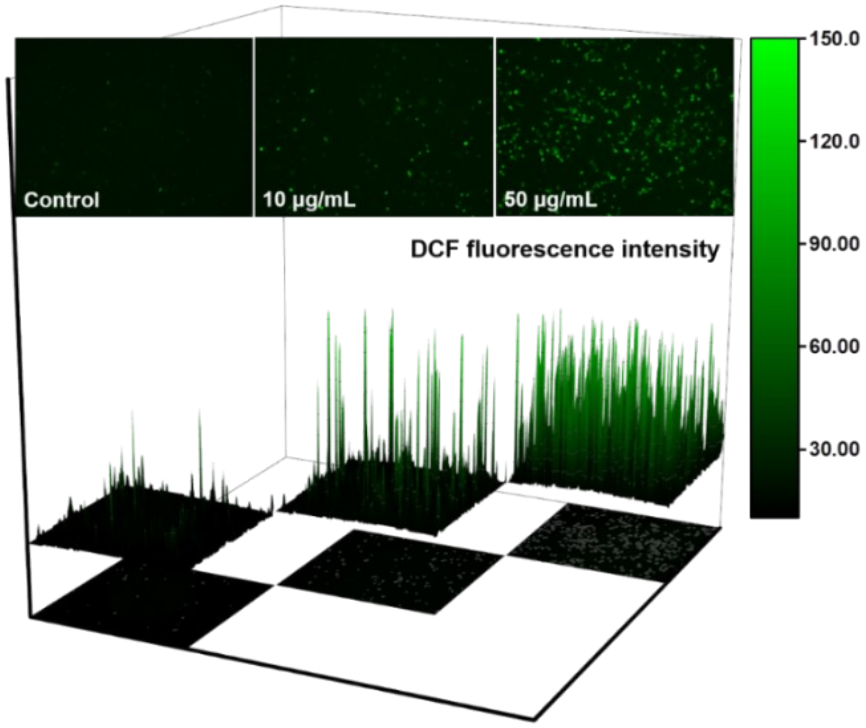

Figure S32. ROS staining images and quantitative analysis of the green fluorescence.

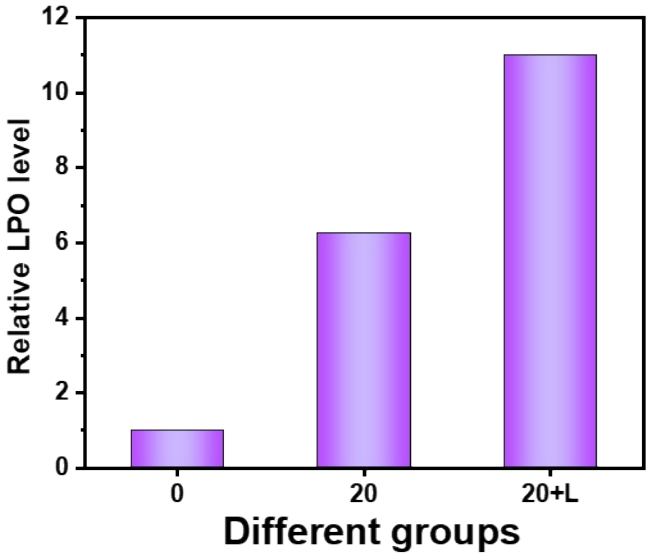

Figure S33. Quantitative analysis of the green fluorescence from LPO staining images of control, 20 μg/mL NPs, 20 μg/mL + Laser irradiation.

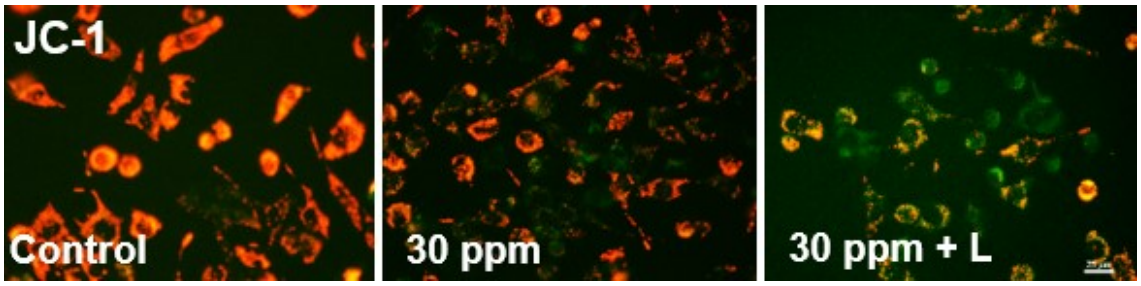

Figure S34. MMP analysis of 4T1 cells incubation with FcNEt-F4 NPs with or without laser irradiation (c = 30 μg/mL).

4. References

(1) P. Hu, K. Du, F. Wei, H. Jiang, C. Kloc, Cryst. Growth Des. **2016**, *16*, 3019-3027.

(2) C. Ou, W. Na, W. Ge, H. Huang, F. Gao, L. Zhong, Y. Zhao, X. Dong, *Angew. Chem. Int. Ed.* **2021**, *60*, 8157-8163.

(3) W. Ge, Y. Xu, C. Liu, W. Xu, Y. Zhang, W. Si, W. Zhao, C. Ou, X. Dong, *J. Mater. Chem. B* **2021**, *9*, 8300-8307.

5. Author Contributions

Prof. X. Dong and Prof. W. Si designed the experiment, supervised the work and revised the manuscript. W. Ge and C. Ou investigated and performed the experiments and wrote the draft. W. Ge, C. Liu, Y. Xu, J. Zhang and W. Wang analyzed and discussed the experimental data. All the authors declare no conflict of interests.